Acta Pharmaceutica Sinica B 2020;10(8):1576–1585

Chinese Pharmaceutical Association
Institute of Materia Medica, Chinese Academy of Medical Sciences

Acta Pharmaceutica Sinica B

www.elsevier.com/locate/apsb
www.sciencedirect.com

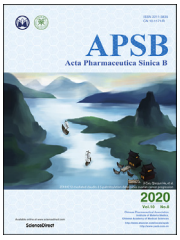

ORIGINAL ARTICLE

Comparative study of mucoadhesive and mucus-penetrative nanoparticles based on phospholipid complex to overcome the mucus barrier for inhaled delivery of baicalein

Wujun Dong[a,b,†], Jun Ye[a,b,†], Junzhuo Zhou[a,b], Weijue Wang[a,b], Hongliang Wang[a,b], Xu Zheng[c], Yanfang Yang[a,b], Xuejun Xia[a,b], Yuling Liu[a,b,*]

[a]*State Key Laboratory of Bioactive Substance and Function of Natural Medicines, Institute of Materia Medica, Chinese Academy of Medical Sciences & Peking Union Medical College, Beijing 100050, China*
[b]*Beijing Key Laboratory of Drug Delivery Technology and Novel Formulation, Institute of Materia Medica, Chinese Academy of Medical Sciences & Peking Union Medical College, Beijing 100050, China*
[c]*State Key Laboratory of Nonlinear Mechanics, Institute of Mechanics, Chinese Academy of Sciences, Beijing 100190, China*

Received 6 August 2019; received in revised form 7 September 2019; accepted 26 September 2019

KEY WORDS

Nanoparticles;
Inhaled delivery;
Mucus-penetrative;
Mucoadhesive;
Baicalein

Abstract Efficient mucosal delivery remains a major challenge for the reason of the respiratory tract mucus act as a formidable barrier to nanocarriers by trapping and clearing foreign particulates. The surface property of nanoparticles determines their retention and penetration ability within the respiratory tract mucus. However, the interaction between nanoparticles and mucus, and how these interactions impact distribution has not been extensively investigated. In this study, polymeric nanoparticles loaded with a baicalein–phospholipid complex were modified with two kinds of polymers, mucoadhesive and mucus-penetrative polymer. Systematic investigations on the physicochemical property, mucus penetration, transepithelial transport, and tissue distribution were performed to evaluate the interaction of nanoparticles with the respiratory tract. Both nanoparticles had a similar particle size and good biocompatibility, exhibited a sustained-release profile, but showed a considerable difference in zeta potential. Interestingly, mucus-penetrative nanoparticles exhibited a higher diffusion rate in mucus, deeper penetration across the mucus layer, enhanced *in vitro* cellular uptake, increased drug distribution in

*Corresponding author. Tel: +86 10 89285188; fax: +86 10 89285190.
E-mail address: ylliu@imm.ac.cn (Yuling Liu).
[†]These authors made equal contributions to this work.
Peer review under the responsibility of Chinese Pharmaceutical Association and Institute of Materia Medica, Chinese Academy of Medical Sciences.

https://doi.org/10.1016/j.apsb.2019.10.002

airways, and superior local distribution and bioavailability as compared to mucoadhesive nanoparticles. These results indicate the potential of mucus-penetrative nanoparticles in design of a rational delivery system to improve the efficiency of inhaled therapy by promoting mucus penetration and increasing local distribution and bioavailability.

1. Introduction

Inhaled drug delivery has great potential for the treatment of various pulmonary conditions such as tuberculosis, asthma, chronic obstructive pulmonary disease, and pulmonary infection. This route of delivery helps in the direct and efficient delivery of high doses of drugs to the target site while reducing systemic exposure and side effects, and avoiding first-pass hepatic metabolism[1−4]. Despite these substantial advantages, the therapeutic efficacy and clinical application of inhaled delivery of relatively small therapeutics are primarily hampered by multiple challenges, including rapid clearance from the site of action, poor accumulation in terminal airways, especially inefficient penetration through the mucosal and epithelial barriers, thereby necessitating more frequent doses of drug[3]. To overcome the aforementioned limitations of conventional immediate-release inhaled formulations, inhaled delivery of therapeutic agents *via* nanocarriers holds great potential owing to the ability to encapsulate drugs and sustain their release, prolong the residence of the payloads within the respiratory tract, and deeply penetrate the mucosal and epithelial barriers[3,5−8]. Amongst the diverse nanocarriers for inhaled delivery, nanoparticles made of biodegradable and biocompatible polymers including polylactic-*co*-glycolic acid, chitosan, and polylactic acid are fitting choices because they show greater encapsulation, good surface engineering properties, and controlled release of drugs for a longer duration[5,9−12].

It is a prerequisite for nanocarriers to penetrate the respiratory tract mucus in order to efficiently deliver drugs to the mucosal surfaces. Evidence suggests that the respiratory tract mucus is a particularly formidable barrier to inhaled delivery of nanocarriers as the mucus has evolved to protect the underlying tissues by efficiently trapping and rapidly clearing foreign particulates[13,14]. The surface property of nanoparticles strongly determines their retention and penetration ability within the respiratory tract and permeation efficiency through the mucus and epithelium[15]. Most modification strategies to improve their effectiveness have focused on coating the nanoparticles with mucoadhesive polymers, such as chitosan[10,11,16,17]. Chitosan is a biocompatible and biodegradable polymer characterized by mucoadhesive property which enables it to interact with the negatively charged mucus that can prolong its residence in the respiratory tract[10,16]. However, mucoadhesive nanoparticles were generally captured in the luminal mucus layer and then largely swept away from the respiratory tract by the mucociliary escalator and expiratory clearance, which compromises their sustained release potential[13]. According to this principle, nanoparticles should be modified to avoid mucoadhesion in the rapidly cleared luminal gel layer and penetrate readily across the slowly cleared periciliary layer, thereby maximizing residence time in the lung[13]. Surface modification by hydrophilic and electro-neutral polymers, such as polyethylene glycol (PEG) and Pluronic F127, has been reported to facilitate the penetration of nanoparticles across highly viscoelastic mucus by minimizing adhesive interactions between nanoparticles and mucus constituents[13,15,18,19]. Although polymeric nanoparticles modified with different types of polymers have been explored for inhaled delivery, very few studies have studied the interaction between polymeric nanoparticles and mucus, and how these interactions impact distribution.

Baicalein, a natural bioactive flavonoid isolated from the root of *Scutellaria baicalensis* Georgi, has been reported to exhibit multiple pharmacological properties, especially anti-viral, anti-inflammatory, and anti-bacterial, making it an attractive candidate for the inhalation treatment of respiratory disorders[20,21]. However, the application of baicalein in the pharmaceutical field and clinical inhalation therapy was limited due to its poor hydrophilicity, lipophilicity, and permeability[21]. As polymeric nanoparticles have been reported to possess many advantages for pulmonary delivery, exploration of inhalable nanoparticles for the delivery of baicalein will be expected to overcome the limitations of conventional aerosol formulations and bypass the physiological barriers in the respiratory tract. However, baicalein is a poorly hydrophilic and lipophilic compound that cannot be loaded effectively into polymeric nanoparticles. In our previous studies, the baicalein−phospholipid complex was successfully developed to improve the lipid solubility of baicalein and then easily associate it with nanocarriers[22,23].

To improve the efficacy of baicalein for the inhalation treatment of respiratory disorders, polymeric nanoparticles loaded with the baicalein−phospholipid complex were developed in this study (Fig. 1). As the surface properties of polymeric nanoparticles have an important effect on the interactions between nanocarriers and the mucus within the respiratory tract, the intrinsic impact of polymers used for surface modification on the distribution and penetration efficiency of polymeric nanoparticles is one of the most critical issues in nanomedicine for promoting effective inhalation therapy. Herein, a systematic investigation was performed to make a comparative evaluation of the interaction of the respiratory tract with polymeric nanoparticles modified with two kinds of polymers: a mucoadhesive polymer (chitosan) and a mucus-penetrative polymer (F127). Physicochemical properties, mucus penetration, and transepithelial transport *in vitro*, and tissue distribution *in vivo* were observed. The study findings will facilitate the design and development of strategies to enhance the efficacy of inhalation therapy.

2. Materials and methods

2.1. Materials

Baicalein (purity 98%) was provided by Jiangsu Zelang Medical Technology Co., Ltd. (Nanjing, China). Baicalein and baicalin

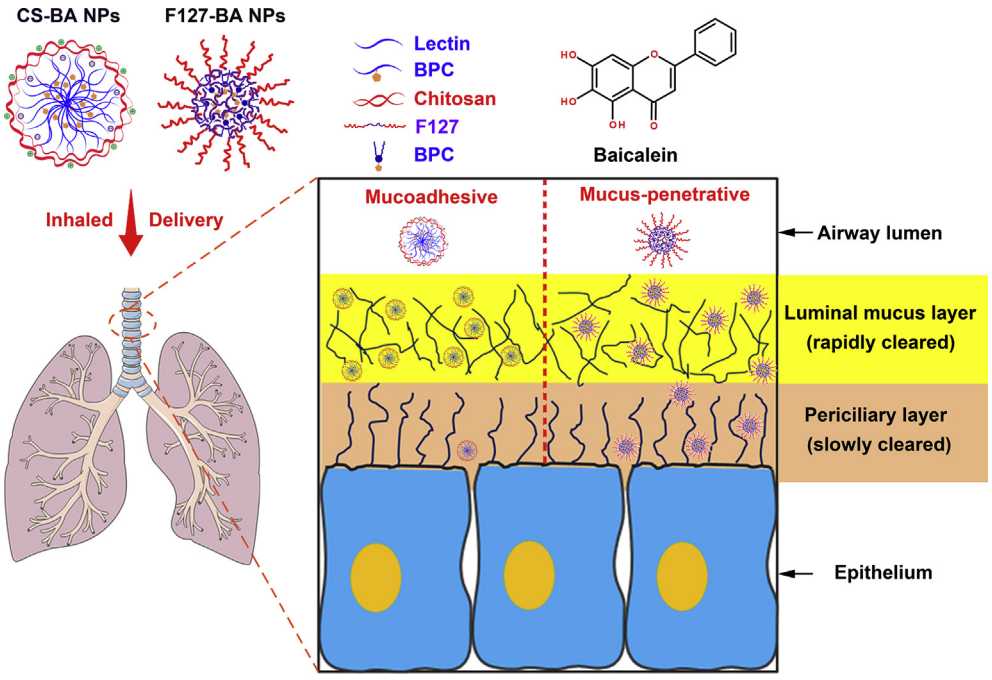

Figure 1 Schematic illustration of the fate of mucoadhesive CS-BA NPs and mucus-penetrative F127-BA NPs upon deposition onto the respiratory tract.

reference substance were purchased from the National Institutes for Food and Drug Control (Beijing, China). Chitosan was purchased from Sigma−Aldrich (St. Louis, MO, USA). Pluronic F127 was provided by BASF (Ludwigshafen, Germany). Egg yolk lecithin (PC-98T) was purchased from A.V.T. Pharmaceutical Co., Ltd. (Shanghai, China). 1,2-dimyristoyl-*sn*-glycero-3-phosphoethanolamine-*N*-(lissamine rhodamine B sulfonyl) (ammonium salt) (Rhodamine-PE) was purchased from Avanti Polar Lipids (Alabaster, AL, USA). Dulbecco's modified Eagle's medium (DMEM) and fetal bovine serum (FBS) were purchased from GE Healthcare (Waukesha, WI, USA). Penicillin-streptomycin, L-glutamine and non-essential amino acids were purchased from Thermo Fisher Scientific (Waltham, MA, USA). All other organic reagents were of analytical grade and purchased from Sinopharm Chemical Reagent Co., Ltd. (Shanghai, China).

2.2. *Cell culture*

Human bronchial epithelial cancer Calu-3 cell line was purchased from the Cell Resource Center, Peking Union Medical College (Beijing, China). Calu-3 cells were grown in DMEM supplemented with 10% FBS, 100 U/mL penicillin, 100 μg/mL streptomycin, 1% non-essential amino acids, and 2 mmol/L L-glutamine in a humidified atmosphere of 5% CO_2 at 37 °C.

2.3. *Preparation of baicalein−phospholipid complex (BPC)*

BPC was prepared using a solvent evaporation method[22]. In brief, baicalein and phospholipids (1:3.5, *w*/*w*) were dissolved in tetrahydrofuran. A solid product, *i.e.*, BPC, was obtained after the organic solvent was totally removed under agitation and vacuum. The resulting BPC was weighed (MS104S; Mettler-Toledo GmbH, Zurich, Switzerland) and stored in a desiccator at room temperature. Fluorescence-labeled BPC was prepared by adding Rhodamine-PE during the preparation of BPC as described above by dissolving Rhodamine-PE (0.25%, *w*/*w*) alongside baicalein and phospholipids in tetrahydrofuran.

2.4. *Preparation and characterization of nanoparticles*

Chitosan-modified nanoparticles (CS-BA NPs) were prepared following the solvent-injection method reported previously[24]. Briefly, chitosan was dissolved in 1% (*v*/*v*) acetic acid and aliquots of this solution were added to 5% (*w*/*v*) Tween-80. BPC was dissolved in ethanol (25 mg/mL) and then added to the ethanolic solution of 2.5% (*w*/*v*) lecithin. Then, CS-BA NPs were obtained by injecting BPC dissolved in lecithin solution into the chitosan solution with continuous moderate stirring for 30 min at room temperature. Finally, the organic solvent was evaporated under vacuum to obtain the resulting CS-BA NPs. Pluronic F127-modified nanoparticles (F127-BA NPs) were prepared by high-pressure homogenization. First, BPC was added to the aqueous phase containing Pluronic F127 (1%, *w*/*v*) with high shear mixing. Then, the mixture was homogenized by high pressure microfluidization homogenizer (Nano DeBEE; BEE International, South Easton, MA, USA) under 14,500 psi for 12 cycles to obtain the resulting F127-BA NPs. Fluorescence-labeled nanoparticles were prepared using a similar procedure with the exception of fluorescence-labeled BPC being dissolved in ethanol with the lipids.

The mean particle size, size distribution and zeta potentials of nanoparticles were measured by the dynamic light scattering method using the zeta potential/particle sizer NICOMP 380 ZLS (PSS NICOMP, Santa Barbara, CA, USA) after appropriate dilution with ultrapure water. Particle morphology was evaluated by transmission electron microscopy (TEM, SU8010; Hitachi, Tokyo, Japan). Samples were prepared by adding 1 drop of nanoparticle suspension to a copper grid followed by staining with 2% (*w*/*v*) phosphotungstic acid. The samples were left to dry and examined.

The stability of nanoparticles was monitored at 4 °C for 1 month. The appearance, mean particle size, size distribution, zeta potentials, content, and entrapment efficiency were determined to evaluate the stability of nanoparticles.

2.5. Entrapment efficiency

The entrapment efficiency of baicalein was determined by a minicolumn centrifugation method[25]. The minicolumn filled with Sephadex G50 was loaded with 0.2 mL nanoparticles and centrifuged at 500 rpm for 1 min (LDZ5-2; Beijing Medical Centrifuge Factory, Beijing, China). After centrifugation, the minicolumn was eluted thrice with 0.5 mL of water to elute the vesicles (1000 rpm for 1 min, LDZ5-2). The eluted baicalein-loaded nanoparticles were collected and the content of entrapped baicalein was determined using high-performance liquid chromatography (HPLC, Agilent 1200; Agilent Technologies, Santa Clara, CA, USA) by disrupting the eluted vesicles with ethanol. Entrapment efficiency (EE, %) was calculated using Eq. (1):

$$\text{EE}\,(\%) = \text{Entrapped drug} \,/\, \text{Total drug} \times 100 \quad (1)$$

2.6. In vitro release

The *in vitro* release profile of baicalein from nanoparticles was assessed in 0.5% (*w*/*v*) Tween-80 in phosphate buffer saline (PBS, pH 7.4) using a dialysis technique. The baicalein-loaded nanoparticles (1 mL) were enclosed in a dialysis bag (MWCO cut-off 8−12 kDa) and immersed in 100 mL of release medium at 37 °C on a shaker (100 rpm; SW22, JULABO GmbH, Seelbach, Germany). At predetermined time points, 1 mL of release medium was withdrawn and replaced with fresh release medium. The samples were filtered through a 0.22 μm membrane filter and analyzed for baicalein content using HPLC. Each sample was performed in triplicate.

2.7. Multiple particle tracking

Fresh pig tracheal mucus was harvested, decontaminated and transferred into centrifuge tubes and stored at 4 °C for use within 24 h of collection.

The tracking of fluorescently labeled nanoparticles in the mucus was performed using multiple particle tracking (MPT)[14,18,26]. Fluorescently labeled nanoparticles (2 μL) at suitable dilution was added to 160 μL tracheal mucus and gently shake for 20 min prior to microscopy. The equilibrated sample was dropped onto a cover glass and movement of particles in the mucus was observed under an inverted fluorescence microscope. Videos were captured at a temporal resolution of 70 ms for 20 s. At least 3 independent experiments were performed while trajectories of $n \geq 100$ particles were analyzed for each experiment. Tracking videos were analyzed using Video Spot Tracking to extract the x and y positional data over time. Time averaged mean square displacement (MSD) was calculated as a function of time scale.

2.8. Cell viability assay

The *in vitro* cytotoxicity of nanoparticles was evaluated in Calu-3 cells using CCK-8 kits (Dojindo Laboratories, Tokyo, Japan). Calu-3 cells were plated at a density of 1×10^4 cells per well in a 96-well plate. After 24 h, the cells were treated with nanoparticles containing various concentrations of baicalein (0, 0.2, 1, 5, 10, 20, and 50 μg/mL). After 2 h of incubation at 37 °C, the number of viable cells was determined using CCK-8 kits according to the manufacturer's protocol. Untreated cells were used as the control and were considered to be 100% viable.

2.9. Establishment and characterization of Calu-3 cell monolayer

To study the epithelial barrier permeability and cellular uptake, the Calu-3 cell monolayer was established by air−liquid interface culture (AIC) system[27,28]. Calu-3 cells were seeded on 12-well Transwell® plates (0.4 μm pore size, 1.12 cm^2 surface area, Costar Corning; Corning, NY, USA) at a density of 2×10^5 cells/well with 0.5 mL in the apical chamber and 1.5 mL medium in the basolateral chamber. After incubation for 2 days, the medium was removed from the apical compartment to allow cells to grow at an air-interface. The medium in the basolateral chamber was changed every 2 days. After 14−17 days, the transepithelial electrical resistance (TEER) was determined by Millicell®-ERS (Millipore, Billerica, MA, USA) to monitor the integrity of the cell monolayer. Only the wells of cell monolayers with stable TEER value above 300 $\Omega \cdot cm^2$ were used for the subsequent uptake and transepithelial transport study.

In order to qualitatively observe the mucus expression profile, the differentiated Calu-3 cell monolayer was washed thrice with cold Hank's balanced salt solution (HBSS), fixed with 4% paraformaldehyde (PFA), stained with Alexa Fluor 488-labeled wheat germ agglutinin (Invitrogen, Molecular Probes, Thermo Fisher Scientific, Waltham, MA, USA), placed on the glass-bottomed cell culture dishes (NEST Biotechnology, Wuxi, China), and observed with confocal laser scanning microscopy (CLSM; FV1000, Olympus, Tokyo, Japan).

2.10. In vitro uptake study of nanoparticles

Prior to the uptake experiment, the medium in the apical and basolateral chambers was discarded and the cells were equilibrated with pre-warmed HBSS for 30 min at 37 °C. For quantitative analysis using HPLC, 0.5 mL of nanoparticles at a baicalein concentration of 40 μg/mL in HBSS and 1.5 mL HBSS were added to the apical and basolateral chambers, respectively. After incubation for 1 h at 37 °C, the cells were washed thrice with cold HBSS, collected, and centrifuged to obtain cell pellets. The baicalein concentration of cell pellets was determined using HPLC. For qualitative analysis using CLSM, 0.5 mL rhodamine-labeled nanoparticles diluted with HBSS and 1.5 mL HBSS were added to the apical and basolateral chambers, respectively. After incubation for 1 h at 37 °C, the cells were washed thrice with cold HBSS, fixed with 4% PFA, stained with DAPI (Beyotime Biotechnology, Shanghai, China), and observed with CLSM.

2.11. Interaction between nanoparticles and mucus during transepithelial transport

In order to assess the interaction between nanoparticles and the mucus which covers the confluent monolayers, the transepithelial transport process of nanoparticles was investigated using the Calu-3 monolayer cultured on Transwells. After equilibration with pre-warmed HBSS for 30 min, the differentiated Calu-3 cell monolayer was exposed to rhodamine-labeled nanoparticles for 6 h at

37 °C. Then the cells were washed thrice with cold HBSS, fixed with 4% PFA, stained with Alexa Fluor 488-labeled wheat germ agglutinin, and observed with CLSM.

2.12. *Pharmacokinetic study*

Male Kunming mice weighing 16−18 g were supplied by Beijing HFK BioScience Co., Ltd. (Beijing, China). All animal experiments were approved by the Institutional Animal Care and Use Committee of Peking Union Medical College. The care of laboratory animal and animal experimental operation was performed in accordance with the Beijing Administration Rule of Laboratory Animal. The mice were randomly divided into three groups for six time points study (n = 90; 5 animals per time point) to receive baicalein solution, CS-BA NPs, and F127-BA NPs at a dose of 18 mg/kg *via* aerosol inhalation treatment. After the completion of administration, the mice of each group (5 animals per time point) were sacrificed at the predetermined time points (5, 15, 30, 60, 120 and 240 min) and lungs were collected, washed with PBS, and stored at −20 °C until analysis. The concentration of baicalein and baicalin in lungs was determined by HPLC−MS/MS (6480B; Agilent Technologies, Santa Clara, CA, USA).

2.13. *Distribution in mouse airways*

Mice were randomly divided into two groups to receive CS-BA NPs and F127-BA NPs *via* aerosol inhalation treatment. The mice were sacrificed by cervical dislocation within 10 min of administration and the trachea was harvested and frozen immediately with liquid nitrogen. Transverse cryosections of the trachea were then prepared and observed with CLSM.

2.14. *Statistical analysis*

All data subjected to statistical analyses were obtained from at least three parallel experiments, and the results are expressed as mean ± standard deviation (SD). The statistical analyses were performed using unpaired two-tailed Student's t-test for two groups, and one-way ANOVA for multiple groups with GraphPad Prism version 7.00 for Windows (GraphPad Software, La Jolla, CA, USA). A P value $\leq$ 0.05 was considered statistically significant.

3. Results and discussion

3.1. *Properties and characteristics of nanoparticles*

Phospholipid complexes are known to improve the lipophilicity of drugs as phospholipids have long fatty acid chain (lipophilic part)[29,30]. In previous studies, the baicalein−phospholipid complex (BPC) was developed to be used as an intermediate of nanocarriers with enhanced lipophilicity[22,23]. In this study, nanocarriers loaded with BPC were successfully prepared and evaluated for mucus penetration properties *in vitro* and *in vivo*.

As mucus is a mesh that captures particles in terms of space and viscosity, the size and surface characteristics of nanocarriers play a pivotal role in improving the mucosal delivery efficiency[14]. Thus, it is of great significance to make a comparative evaluation of the interaction of the respiratory tract with polymeric nanoparticles modified with different kinds of polymers. Various types of polymers, such as chitosan and carbomer, have been widely investigated as mucoadhesive materials to modify nanoparticles[31]. A previous study reported the use of Pluronic F68 as a mucoadhesive polymer to coat nanoparticles and made a careful head-to-

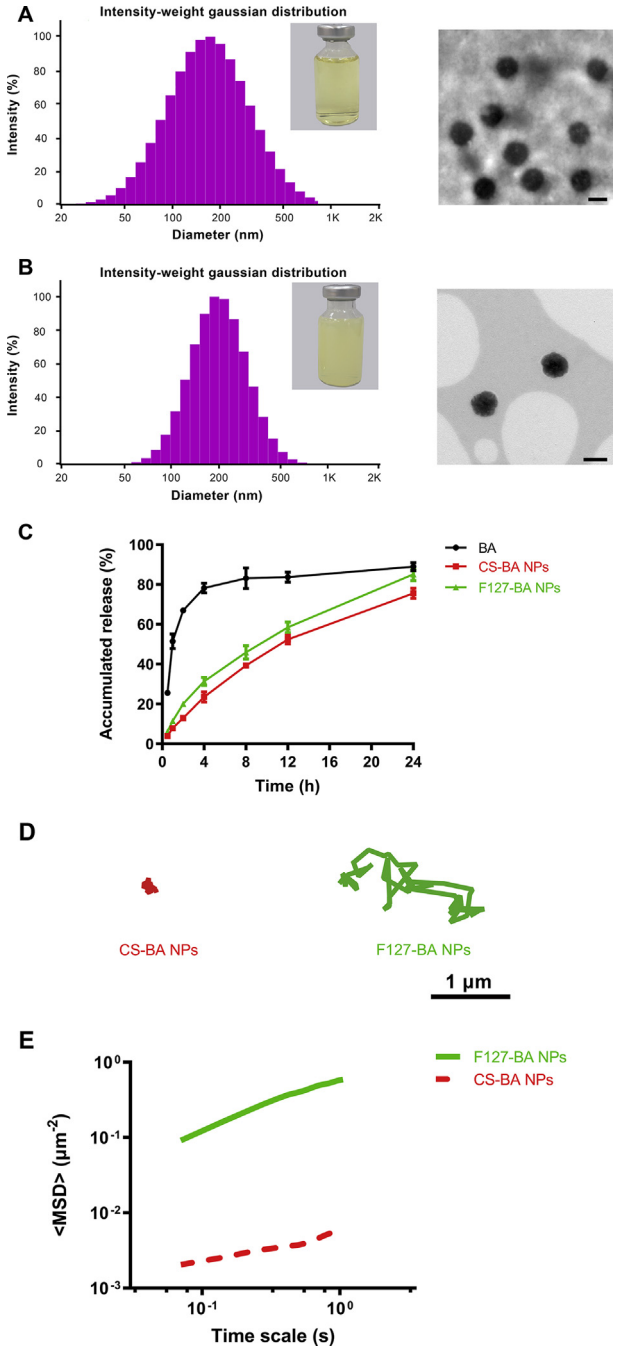

Figure 2 *In vitro* characterization and the diffusion behavior of nanoparticles in respiratory mucus. (A) Particle size distribution, appearance, and morphology of CS-BA NPs; (B) particle size distribution, appearance, and morphology of F127-BA NPs; (C) *in vitro* release profile of nanoparticles in PBS (pH 7.4) containing 0.5% (*w*/*v*) Tween 80. Each value represents the mean ± SD (n = 3). Scale bar = 200 nm; (D) representative trajectories of nanoparticles in respiratory mucus; (E) ensemble-averaged geometric mean squared displacement (<MSD>) as a function of timescale for nanoparticles in respiratory mucus.

head comparison to gain an insight into the *in vivo* behavior of mucoadhesive and mucus-penetrative nanoparticles following inhalation[32]. However, Pluronic F68 is not appropriate to be used as a representative mucoadhesive material due to its dual character, including mucoadhesive and mucus-penetrative properties reported in the literature[14,32–34]. Chitosan, a natural polycationic polymer with mucoadhesive property, is a most frequently used mucoadhesive polymer and can interact with the negatively charged phospholipids to self-assemble nanoparticles, which demonstrate good biocompatibility and biodegradability, excellent mucosal adhesiveness, and minimal cytotoxicity[24,35,36]. In this study, self-assembled chitosan/lecithin nanoparticles, which are composed of a BPC surrounded by a chitosan layer, were prepared by the solvent-injection method. In marked contrast to the mucoadhesive properties of chitosan, Pluronic F127 have been reported to protect the surface of nanoparticles from electrostatic and hydrophobic interactions with mucus and then rapidly penetrate mucus[14]. Based on the concept of mucus-penetrative nanoparticles, nanosuspensions were developed and prepared from BPC and coated with Pluronics F127 to evaluate the efficiency of mucosal delivery.

As shown in Fig. 2A and B, both CS-BA NPs and F127-BA NPs formed a light-yellow translucent emulsion and exhibited a similar mean particle size (202.6 ± 8.9 and 219.9 ± 8.8 nm, respectively) and size distribution. It was reported that mucus secretions have an average mesh size between 140 and 340 nm, with a wide range of size distribution[14]. Therefore, the ~200 nm size of both CS-BA NPs and F127-BA NPs will be beneficial to allow them to diffuse through mucus.

Zeta potential is a factor that not only determines the physical stability of nanocarriers, but also has an important effect on the interaction of nanocarriers with mucus. The zeta potentials of CS-BA NPs and F127-BA NPs were +41.34 ± 0.30 and −7.42 ± 0.81 mV, respectively, which were closely related to the properties of surface modified materials of nanoparticles. Compared to a nonionic polymer F127, the polycationic polymer chitosan possesses a highly positive charge and its adsorption onto the surface appeared to raise the zeta potential of CS-BA NPs significantly from slightly negative to positive values[37]. The high values of zeta potential obtained for CS-BA NPs indicated relatively high surface charges, not only being beneficial for the physical stability, but also being able to interact with the negatively charged mucus of the respiratory tract[38]. TEM examination revealed that the both kinds of nanoparticles were spherical and regular in shape. It should be noted that both CS-BA NPs and F127-BA NPs have a high drug encapsulation efficiency (above 80%), which may be attributed to the enhanced lipophilicity of BPC. The increased solubility of BPC in ethanol enabled successful encapsulation in chitosan/lecithin nanoparticles during the self-assembly process[24].

To evaluate the effect of polymer modification on the stability of nanoparticles, the prepared nanoparticles were stored at 4 °C for 1 month and physicochemical properties were evaluated. The results of the stability tests showed that the appearance, mean particle size, size distribution, zeta potentials, content, and entrapment efficiency of nanoparticles hardly changed within 1 month at 4 °C, indicating that all the nanoparticles exhibited favorable stability.

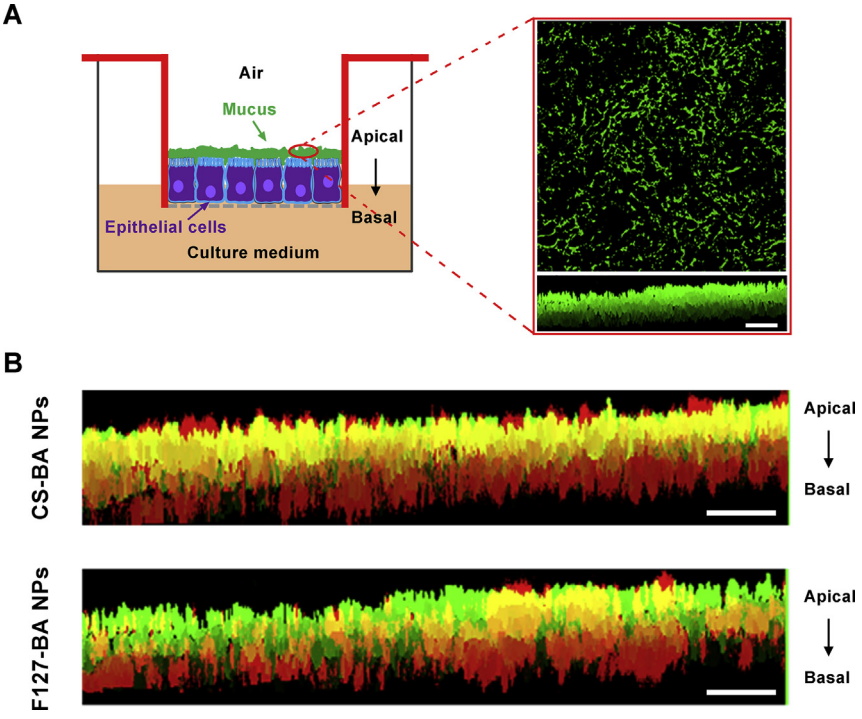

Figure 3 The penetration behavior of nanoparticles in Calu-3 monolayer model. (A) Cartoon illustration of the Calu-3 monolayer model by air–liquid interface culture (AIC) system and confocal laser scanning microscopy (CLSM) images of Calu-3 monolayer model mucus stained with AlexaFluor-488-labeled wheat germ agglutinin (green staining). Scale bar = 50 nm; (B) CLSM images of Calu-3 monolayer model exposed to rhodamine-loaded nanoparticles (red fluorescence) for 6 h and subsequent staining of mucus with AlexaFluor-488-labeled wheat germ agglutinin (green staining). Scale bar = 50 nm.

3.2. *In vitro sustained-release profile of nanoparticles*

As shown in Fig. 2C, the free baicalein exhibited a relatively rapid release feature with more than 80% of drug released from the dialysis bag within 4 h. In comparison, both CS-BA NPs and F127-BA NPs exhibited a similar sustained-release characteristic and the cumulative release was only 23.4% and 31.3% respectively, during the same time period. These results indicate that the nanoparticles based on BPC can not only effectively encapsulate the poorly soluble drug, but also release baicalein in a sustained manner. The sustained-release profile of nanoparticles, which may be associated with the slower diffusion of the baicalein from nanoparticles, could prevent spreading of baicalein over the respiratory tract fluid before diffusing through the mucus, thus leading to effective delivery.

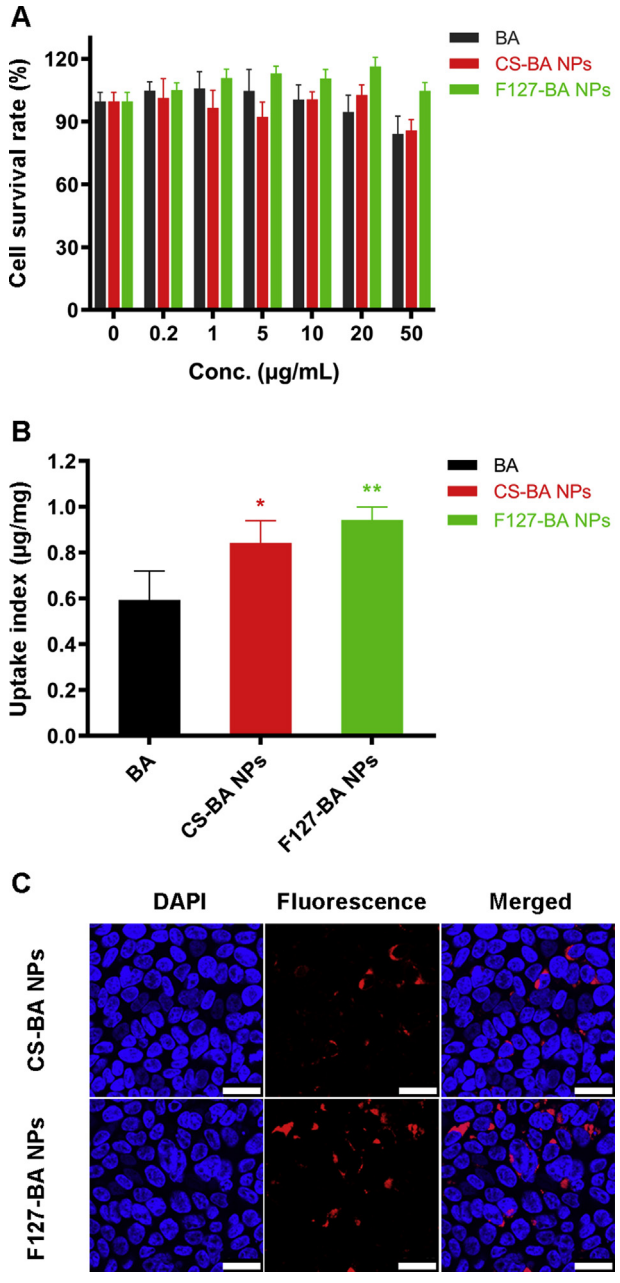

Figure 4 *In vitro* cellular uptake profile of nanoparticles in Calu-3 monolayer model. (A) *In vitro* cytotoxicity of nanoparticles in Calu-3 cells at 2 h. Each value represents the mean ± SD ($n = 5$); (B) the uptake index was determined by HPLC. Each value represents the mean ± SD ($n = 3$). *$P < 0.05$ *vs.* BA, **$P < 0.01$ *vs.* BA; (C) CLSM images of cellular uptake. Scale bar = 25 μm.

3.3. *Diffusion behavior of nanoparticles in respiratory mucus*

Mucus barriers lining the mucosal epithelia could promptly trap and clear away most exogenous nanoparticles from the mucosae and then compromise the efficacy of nanocarrier-based mucosal drug delivery and imaging[39]. To improve the efficacy of mucosal delivery, nanocarriers must be capable of fast mobility and diffuse through the highly protective mucus linings[39]. Therefore, the diffusion behavior in respiratory mucus is a pivotal parameter to evaluate the penetrability of nanocarriers. Additionally, investigation of the diffusion in mucus could provide corroborative evidence for the effectiveness of surface coatings at reducing interactions with mucus[14].

A comparative evaluation was first made of the transport behavior of CS-BA NPs and F127-BA NPs in fresh respiratory mucus using multiple particle tracking (MPT). As shown in Fig. 2D, CS-BA NPs exhibited highly hindered trajectories and were nearly immobilized in the mucus. In contrast, the F127-BA NPs trajectories spanned much larger distances and were more diffusive. The MSD is the square of the distance a single particle moves over a given time interval; thus, MSD is proportional to particle diffusion rates[40]. The geometric ensemble-averaged MSD (<MSD>) of at least 100 individual particles of each particle type were calculated to quantify these differences. Greater <MSD> represents faster particle movement. The <MSD> of F127-BA NPs was consistently much greater than that of CS-BA NPs (Fig. 2E). At a time scale of 1 s, the <MSD> of PF127-BA NPs was about 100-fold greater than that of CS-BA NPs. The <MSD> of CS-BA NPs was 2300-fold lower than the theoretical MSD of similarly sized nanoparticles in water at a time scale of 1 s, whereas the <MSD> of F127-BA NPs was only 8.6-fold lower. The results demonstrated that the nanoparticles coated with chitosan exhibited constrained movement in mucus compared to the nanoparticles modified by F127 that traveled greater distances. The different diffusion behaviors of CS-BA NPs and F127-BA NPs in respiratory mucus could be attributed to the different properties of the two surface modification polymers, chitosan and F127. The cationic amino groups of chitosan have mucoadhesive properties and enable chitosan to interact with the negatively charged mucus *via* electrostatic forces[41]. In contrast, hydrophilic and electro-neutral Pluronic F127 could minimize nanoparticle affinity to mucus constituents[33]. Therefore, the higher diffusion rate of F127-BA NPs in mucus will be beneficial in improving the mucus penetration efficiency, and be expected to facilitate prolonged retention of nanoparticles at mucosal surfaces, leading to improved pharmacokinetics and therapeutic efficacy.

3.4. *Mucus penetration ability of nanoparticles*

In order to evaluate the expression level of mucin on the differentiated Calu-3 cell monolayer, the cell-covering mucus layer of a 14−17 days culture of Calu-3 cells was stained with the Alexa-Fluor-488-labeled wheat germ agglutinin[34]. As shown in Fig. 3A, after 14 days of culture using the AIC method, a large amount of mucin was expressed on the surface of the cell layer, which was in

line with the results reported previously[28,34]. Additionally, the TEER value of differentiated Calu-3 cell monolayer exceeded the threshold value (300 $\Omega \cdot cm^2$). Therefore, the established *in vitro* Calu-3 cell model can be used for the subsequent *in vitro* transepithelial transport and cellular uptake study.

In the captured images of CLSM, the green, red, and yellow fluorescence represents the mucus, rhodamine-labeled nanoparticles, and the colocalization of mucus and nanoparticles, respectively. After incubation for 6 h, CS-BA NPs exhibited significantly greater red fluorescence overlapped with green fluorescence (corresponding to the mucus layer) in comparison with F127-BA NPs (Fig. 3B), indicating that CS-BA NPs had a higher binding affinity to mucus than F127-BA NPs. As explained in the results of MPT, the higher binding affinity of CS-BA NPs may be associated with the interaction of the positively charged CS-BA NPs and the negatively charged mucus. Contrary to the mucoadhesive behavior of CS-BA NPs, F127-BA NPs seemed to partly penetrate the mucus layer and reach the surface of the epithelial monolayer. These differences in the transepithelial transport behavior of nanoparticles were in accordance with the particle motion profiles of nanoparticles in fresh respiratory mucus mentioned above.

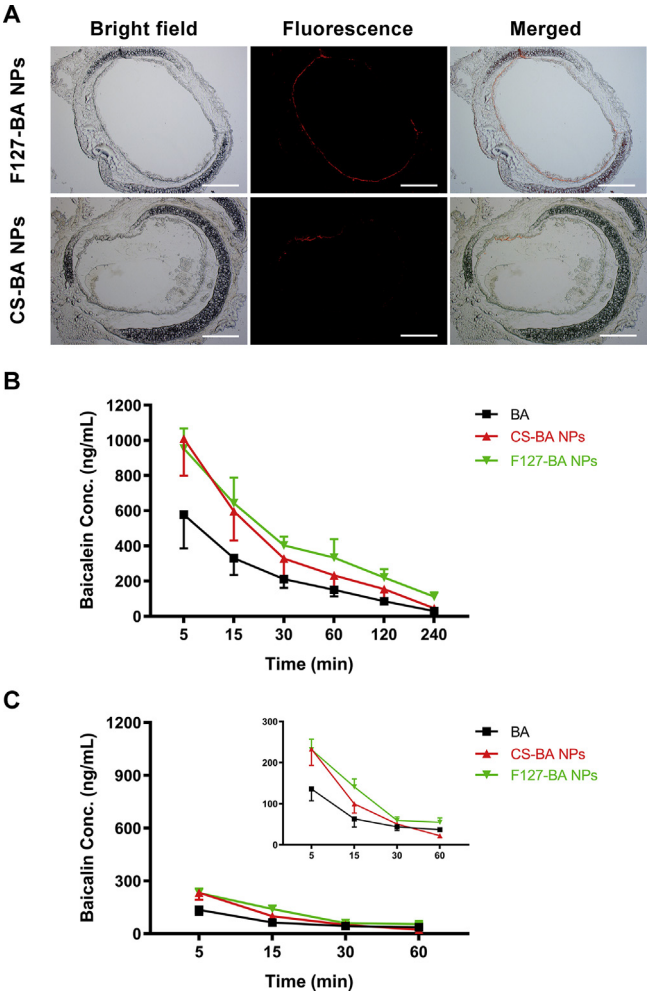

Figure 5 *In vivo* distribution of nanoparticles. (A) Transverse frozen sections of mouse trachea tissue following inhalation administration of rhodamine-labeled nanoparticles. Mean lung concentration−time profiles of baicalein (B) and baicalin (C) after inhalation administration of BA solution, CS-BA NPs, and F127-BA NPs. The inset to Fig. 5C magnifies the *y*-axis. Each value represents the mean ± SD ($n = 5$).

3.5. *In vitro cellular uptake profile of nanoparticles*

The results of the cell viability assay indicated that nanoparticles at a baicalein concentration lower than 50 μg/mL produced negligible Calu-3 cytotoxicity (Fig. 4A), indicating significant biocompatibility of nanoparticles with epithelial cells. Therefore, a concentration of 40 μg/mL baicalein was chosen to study the *in vitro* uptake of nanoparticles.

As shown in Fig. 4B, the uptake index of both CS-BA NPs and F127-BA NPs was greater than that of free baicalein, indicating that nanoparticles loaded with a BPC significantly facilitated the uptake of baicalein by Calu-3 cells. Compared to CS-BA NPs, F127-BA NPs exhibited a trend of enhanced cellular uptake, which was confirmed by the result of CLSM (Fig. 4C). The mucus layer was identified to immobilize and remove cationic nanoparticles (such as CS-BA NPs), the increased cellular uptake of F127-BA NPs may be ascribed to its deeper mucus penetration and the additional accumulation on the surface of epithelial cells (Fig. 3B).

3.6. *Distribution of nanoparticles in mouse airways*

Representative images of transverse sections of the large airways are shown in Fig. 5A. It was found that CS-BA NPs were sparsely distributed throughout the lung airways, whereas F127-BA NPs exhibited more widespread distribution across the epithelial surface. The MPT results mentioned above confirmed that F127-BA NPs exhibited effective particle mobility in comparison with CS-BA NPs in mucus, and the particle mobility in mucus has been proven to correlate with *in vivo* mucosal distribution[39]. Therefore, better particle mobility of F127-BA NPs likely contributed to the increased drug distribution in airways by resisting mucociliary clearance and enhancing mucus penetration.

3.7. *Lung tissue distribution of nanoparticles*

The mean lung concentration−time profiles of baicalein after administration of free baicalein and nanoparticles are shown in Fig. 5B. The primary pharmacokinetic parameters were calculated using Drug and Statistics (DAS) 3.0 software (BioGuider Medicinal Technology Co., Ltd., Shanghai, China) and are summarized in Table 1.

As shown in Fig. 5B, the free baicalein exhibited rapid elimination in mice when dosed at 18 mg/kg. Inhalable nanoparticles for the delivery of active ingredients have been previously reported to extend lung retention and sustain drug release after inhalation[7]. In this study, the baicalein concentration in the lung tissue of both CS-BA NPs and F127-BA NPs groups was significantly higher than that of the free baicalein group at different time points (up to 240 min). Fifteen minutes after initial administration, the baicalein concentration of the CS-BA NPs group was 1.75 times higher than that of the free baicalein group and was comparable with that of F127-BA NPs, which may be ascribed to the adhesion interaction of CS-BA NPs with the mucus layer after inhalation. Interestingly, the F127-BA NPs group exhibited higher baicalein concentration and a certain degree of prolonged drug retention in the lung tissue after more than 15 min as compared to the CS-BA NPs group, indicating that F127-BA NPs have a better lung deposition. As shown in Table 1, pulmonary delivery of

Table 1 Pharmacokinetics parameters of baicalein in lung ($n = 5$).

Parameters	Value		
	BA	CS-BA NPs	F127-BA NPs
$AUC_{(0-t)}$ (ng/g·min)	29,429.3	49,558.8	65,822.3
$AUC_{(0-\infty)}$ (ng/g·min)	32,613.3	54,368.7	84,062.6
$AUMC_{(0-t)}$	1,973,907.9	3,323,580.2	5,318,220.7
$AUMC_{(0-\infty)}$	3,087,672.8	4,993,053.6	12,680,998.8
$MRT_{(0-t)}$ (min)	67.07	67.06	80.80
$MRT_{(0-\infty)}$ (min)	94.68	91.84	150.85
T_{max} (min)	5	5	5
C_{max} (ng/g)	577.03	1009.35	953.98

F127-BA NPs led to about 1.5- to 2.6-fold increase in the area under curve (AUC) in the lung tissues as compared to CS-BA NPs and the free baicalein following the administration procedure. Additionally, a remarkable increase of mean retention time (MRT) was observed in the F127-BA NPs group as compared to the CS-BA NPs and free baicalein group. Compared to the mucoadhesive CS-BA NPs, the modification by hydrophilic material F127 changes the surface chemistry of F127-BA NPs, such that hydrophilicity and electrical neutrality, make the nanoparticles less susceptible to adhesion by mucin in the mucus and enable it to rapidly penetrate the mucus layer, thereby improving the distribution of baicalein in the lungs.

Baicalein is rapidly metabolized to baicalin in the body after intravenous or oral administration[22,42], thereby influencing the pharmacological activity. It is worth mentioning that baicalein is mainly distributed in the lungs with the parent form after inhalation treatment, which may be attributed to the less metabolic enzymes covered on the mucosal surface (Fig. 5C). This result indicated that inhaled delivery of baicalein is beneficial for baicalein to exert the pharmacological activity.

4. Conclusions

In this study, a comparative evaluation of the interaction between mucus and polymeric nanoparticles with different surface functionalization was made, and the impact of these interactions on distribution was assessed. The overall findings indicated that inhalation route of delivery of baicalein *via* mucus-penetrative nanoparticles could deliver the drug with a higher diffusion rate in fresh respiratory mucus, allow deeper penetration into the mucus layer, enhance *in vitro* cellular uptake by the Calu-3 cells, increase drug distribution in airways, and provide superior local distribution and bioavailability as compared to a mucoadhesive formulation with similar particle size. It represents a promising inhalable carrier that can deliver baicalein to the respiratory tract at a reduced dosing frequency.

Acknowledgments

This work was financially supported by National Science and Technology Major Project of China (Grant Nos. 2018ZX09721003 and 2018ZX09711001).

Author contributions

Wujun Dong, Jun Ye, Junzhuo Zhou, Weijue Wang, Hongliang Wang, Xu Zheng, Yanfang Yang, and Xuejun Xia were responsible for study initiation, experimental design, the acquisition and analysis of data, and writing. Yuling Liu developed the hypothesis, reviewed, edited and approved the manuscript for publication.

Conflict of interest

The authors have no conflicts of interest to declare.

Appendix A. Supporting information

Supporting data to this article can be found online at https://doi.org/10.1016/j.apsb.2019.10.002.

References

1. Zhou QT, Leung SS, Tang P, Parumasivam T, Loh ZH, Chan HK. Inhaled formulations and pulmonary drug delivery systems for respiratory infections. *Adv Drug Deliv Rev* 2015;**85**:83–99.
2. Liang Z, Ni R, Zhou J, Mao S. Recent advances in controlled pulmonary drug delivery. *Drug Discov Today* 2015;**20**:380–9.
3. Lim YH, Tiemann KM, Hunstad DA, Elsabahy M, Wooley KL. Polymeric nanoparticles in development for treatment of pulmonary infectious diseases. *Wiley Interdiscip Rev Nanomed Nanobiotechnol* 2016;**8**:842–71.
4. Zhang T, Chen Y, Ge Y, Hu Y, Li M, Jin Y. Inhalation treatment of primary lung cancer using liposomal curcumin dry powder inhalers. *Acta Pharma Sin B* 2018;**8**:440–8.
5. Xu C, Wang Y, Guo Z, Chen J, Lin L, Wu J, et al. Pulmonary delivery by exploiting doxorubicin and cisplatin co-loaded nanoparticles for metastatic lung cancer therapy. *J Control Release* 2019;**295**:153–63.
6. Garbuzenko OB, Kbah N, Kuzmov A, Pogrebnyak N, Pozharov V, Minko T. Inhalation treatment of cystic fibrosis with lumacaftor and ivacaftor co-delivered by nanostructured lipid carriers. *J Control Release* 2019;**296**:225–31.
7. Joshi N. Nanotechnology enabled inhalation of bio-therapeutics for pulmonary diseases: design considerations and challenges. *Curr Pathobiol Rep* 2018;**6**:225–31.
8. Abdelaziz HM, Gaber M, Abd-Elwakil MM, Mabrouk MT, Elgohary MM, Kamel NM, et al. Inhalable particulate drug delivery systems for lung cancer therapy: nanoparticles, microparticles, nanocomposites and nanoaggregates. *J Control Release* 2018;**269**:374–92.
9. Alhajj N, Zakaria Z, Naharudin I, Ahsan F, Li W, Wong TW. Critical physicochemical attributes of chitosan nanoparticles admixed lactose-PEG 3000 microparticles in pulmonary inhalation. *Asian J Pharma Sci* 2020;**15**:374–84.
10. Rawal T, Patel S, Butani S. Chitosan nanoparticles as a promising approach for pulmonary delivery of bedaquiline. *Eur J Pharm Sci* 2018;**124**:273–87.
11. Paul P, Sengupta S, Mukherjee B, Shaw TK, Gaonkar RH, Debnath MC. Chitosan-coated nanoparticles enhanced lung pharmacokinetic profile of voriconazole upon pulmonary delivery in mice. *Nanomedicine* 2018;**13**:501–20.
12. Li C, Wang J, Wang Y, Gao H, Wei G, Huang Y, et al. Recent progress in drug delivery. *Acta Pharma Sin B* 2019;**9**:1145–62.
13. Popov A, Schopf L, Bourassa J, Chen H. Enhanced pulmonary delivery of fluticasone propionate in rodents by mucus-penetrating nanoparticles. *Int J Pharm* 2016;**502**:188–97.
14. Yu T, Chisholm J, Choi WJ, Anonuevo A, Pulicare S, Zhong W, et al. Mucus-penetrating nanosuspensions for enhanced delivery of poorly soluble drugs to mucosal surfaces. *Adv Healthc Mater* 2016;**5**:2745–50.
15. Liu M, Wu L, Zhu X, Shan W, Li L, Cui Y, et al. Core–shell stability of nanoparticles plays an important role for overcoming the intestinal mucus and epithelium barrier. *J Mater Chem B* 2016;**4**:5831–41.

16. Rosière R, Van Woensel M, Gelbcke M, Mathieu V, Hecq J, Mathivet T, et al. New folate-grafted chitosan derivative to improve delivery of paclitaxel-loaded solid lipid nanoparticles for lung tumor therapy by inhalation. *Mol Pharm* 2018;**15**:899−910.
17. Al-Nemrawi NK, Alshraiedeh NH, Zayed AL, Altaani BM. Low molecular weight chitosan-coated PLGA nanoparticles for pulmonary delivery of tobramycin for cystic fibrosis. *Pharmaceuticals* 2018;**11**. pii: E28.
18. Xu Q, Boylan NJ, Cai S, Miao B, Patel H, Hanes J. Scalable method to produce biodegradable nanoparticles that rapidly penetrate human mucus. *J Control Release* 2013;**170**:279−86.
19. Lai SK, Wang YY, Hanes J. Mucus-penetrating nanoparticles for drug and gene delivery to mucosal tissues. *Adv Drug Deliv Rev* 2009;**61**: 158−71.
20. Dinda B, Dinda S, Das Sharma S, Banik R, Chakraborty A, Dinda M. Therapeutic potentials of baicalin and its aglycone, baicalein against inflammatory disorders. *Eur J Med Chem* 2017;**131**:68−80.
21. Zhang J, Lv H, Jiang K, Gao Y. Enhanced bioavailability after oral and pulmonary administration of baicalein nanocrystal. *Int J Pharm* 2011; **420**:180−8.
22. Zhou Y, Dong W, Ye J, Hao H, Zhou J, Wang R, et al. A novel matrix dispersion based on phospholipid complex for improving oral bioavailability of baicalein: preparation, *in vitro* and *in vivo* evaluations. *Drug Deliv* 2017;**24**:720−8.
23. Meng L, Xia X, Yang Y, Ye J, Dong W, Ma P, et al. Co-encapsulation of paclitaxel and baicalein in nanoemulsions to overcome multidrug resistance *via* oxidative stress augmentation and P-glycoprotein inhibition. *Int J Pharm* 2016;**513**:8−16.
24. Liu L, Zhou C, Xia X, Liu Y. Self-assembled lecithin/chitosan nanoparticles for oral insulin delivery: preparation and functional evaluation. *Int J Nanomed* 2016;**11**:761−9.
25. Ye J, Dong W, Yang Y, Hao H, Liao H, Wang B, et al. Vitamin E-rich nanoemulsion enhances the antitumor efficacy of low-dose paclitaxel by driving Th1 immune response. *Pharm Res* 2017;**34**:1244−54.
26. Shan W, Zhu X, Liu M, Li L, Zhong J, Sun W, et al. Overcoming the diffusion barrier of mucus and absorption barrier of epithelium by self-assembled nanoparticles for oral delivery of insulin. *ACS Nano* 2015; **9**:2345−56.
27. Asai A, Okuda T, Sonoda E, Yamauchi T, Kato S, Okamoto H. Drug permeation characterization of inhaled dry powder formulations in air−liquid interfaced cell layer using an improved, simple apparatus for dispersion. *Pharm Res* 2016;**33**:487−97.
28. Grainger CI, Greenwell LL, Lockley DJ, Martin GP, Forbes B. Culture of Calu-3 cells at the air interface provides a representative model of the airway epithelial barrier. *Pharm Res* 2006;**23**:1482−90.
29. Li B, Han L, Cao B, Yang X, Zhu X, Yang B, et al. Use of magnoflorine−phospholipid complex to permeate blood−brain barrier and treat depression in the CUMS animal model. *Drug Deliv* 2019;**26**: 566−74.
30. Fan J, Dai Y, Shen H, Ju J, Zhao Z. Application of soluplus to improve the flowability and dissolution of baicalein phospholipid complex. *Molecules* 2017;**22**. pii E776.
31. Netsomboon K, Bernkop-Schnürch A. Mucoadhesive *vs.* mucopenetrating particulate drug delivery. *Eur J Pharm Biopharm* 2016;**98**:76−89.
32. Schneider CS, Xu Q, Boylan NJ, Chisholm J, Tang BC, Schuster BS, et al. Nanoparticles that do not adhere to mucus provide uniform and long-lasting drug delivery to airways following inhalation. *Sci Adv* 2017;**3**:e1601556.
33. Yang M, Lai SK, Wang YY, Zhong W, Happe C, Zhang M, et al. Biodegradable nanoparticles composed entirely of safe materials that rapidly penetrate human mucus. *Angew Chem Int Ed Engl* 2011;**50**: 2597−600.
34. Mura S, Hillaireau H, Nicolas J, Kerdine-Römer S, Le Droumaguet B, Deloménie C, et al. Biodegradable nanoparticles meet the bronchial airway barrier: how surface properties affect their interaction with mucus and epithelial cells. *Biomacromolecules* 2011;**12**:4136−43.
35. M Ways TM, Lau WM, Khutoryanskiy VV. Chitosan and its derivatives for application in mucoadhesive drug delivery systems. *Polymers* 2018;**10**. pii E267.
36. Xu J, Strandman S, Zhu JX, Barralet J, Cerruti M. Genipin-crosslinked catechol-chitosan mucoadhesive hydrogels for buccal drug delivery. *Biomaterials* 2015;**37**:395−404.
37. Chen D, Xia D, Li X, Zhu Q, Yu H, Zhu C, et al. Comparative study of Pluronic® F127-modified liposomes and chitosan-modified liposomes for mucus penetration and oral absorption of cyclosporine A in rats. *Int J Pharm* 2013;**449**:1−9.
38. Mitri K, Shegokar R, Gohla S, Anselmi C, Müller RH. Lipid nanocarriers for dermal delivery of lutein: preparation, characterization, stability and performance. *Int J Pharm* 2011;**414**:267−75.
39. Yu T, Chan KW, Anonuevo A, Song X, Schuster BS, Chattopadhyay S, et al. Liposome-based mucus-penetrating particles (MPP) for mucosal theranostics: demonstration of diamagnetic chemical exchange saturation transfer (diaCEST) magnetic resonance imaging (MRI). *Nanomedicine* 2015;**11**:401−5.
40. Osman G, Rodriguez J, Chan SY, Chisholm J, Duncan G, Kim N, et al. PEGylated enhanced cell penetrating peptide nanoparticles for lung gene therapy. *J Control Release* 2018;**285**:35−45.
41. Al-Obaidi H, Kalgudi R, Zariwala MG. Fabrication of inhaled hybrid silver/ciprofloxacin nanoparticles with synergetic effect against *Pseudomonas aeruginosa*. *Eur J Pharm Biopharm* 2018;**128**:27−35.
42. Lai MY, Hsiu SL, Tsai SY, Hou YC, Chao PD. Comparison of metabolic pharmacokinetics of baicalin and baicalein in rats. *J Pharm Pharmacol* 2003;**55**:205−9.